JOURNAL OF GEOPHYSICAL RESEARCH, VOL. 106, NO. C1, PAGES 899-915, JANUARY 15, 2001

Satellite-measured chlorophyll and temperature variability off northern Chile during the 1996-1998 La Niña and El Niño

A. C. Thomas,[1] J. L. Blanco,[2] M. E. Carr,[3] P. T. Strub,[4] and J. Osses[2]

Abstract. Time series of satellite measurements are used to describe patterns of surface temperature and chlorophyll associated with the 1996 cold La Niña phase and the 1997-1998 warm El Niño phase of the El Niño – Southern Oscillation cycle in the upwelling region off northern Chile. Surface temperature data are available through the entire study period. Sea-viewing Wide Field-of-view Sensor (SeaWiFS) data first became available in September 1997 during a relaxation in El Niño conditions identified by in situ hydrographic data. Over the time period of coincident satellite data, chlorophyll patterns closely track surface temperature patterns. Increases both in nearshore chlorophyll concentration and in cross-shelf extension of elevated concentrations are associated with decreased coastal temperatures during both the relaxation in El Niño conditions in September-November 1997 and the recovery from El Niño conditions after March 1998. Between these two periods during austral summer (December 1997 to March 1998) and maximum El Niño temperature anomalies, temperature patterns normally associated with upwelling were absent and chlorophyll concentrations were minimal. Cross-shelf chlorophyll distributions appear to be modulated by surface temperature frontal zones and are positively correlated with a satellite-derived upwelling index. Frontal zone patterns and the upwelling index in 1996 imply an austral summer nearshore chlorophyll maximum, consistent with SeaWiFS data from 1998-1999, after the El Niño. SeaWiFS retrievals in the data set used here are higher than in situ measurements by a factor of 2-4; however, consistency in the offset suggests relative patterns are valid.

1. Introduction

Equatorward wind stress along the northern coast of Chile (Figure 1) produces upwelling, relatively cold coastal surface temperatures, and a biologically productive region, which supports a strong commercial fishery. A climatology of seasonal hydrographic patterns for the region recently compiled by *Blanco et al.* [2000] shows that upwelling occurs year round, consistent with the assessment of *Fonseca and Farias* [1987] and patterns shown by *Rojas and Silva* [1996]. Climatological isotherms and isohalines tilt upward toward the coast accompanied by equatorward surface geostrophic flow throughout the year. Strongest upwelling and cross-shelf gradients occur in austral summer (January, February, and March) in concert with the local seasonal maximum in both equatorward alongshore wind stress and solar heating of surface water. Weakest alongshore wind stress, gradients, and upwelling occur in austral winter. Synoptic phytoplankton patterns in the region are less well known, but previous work suggests a general trend consistent with the hydrographic patterns. Using field data from two seasons, *Morales et al.* [1996] show winter cross-shelf chlorophyll concentrations and temperature patterns are relatively heterogeneous with concentrations > 1.0 mg m^{-3} extending at least 100 km offshore. In spring, cross-shelf gradients are enhanced, and the region of increased biological activity (chlorophyll > 1.0 mg m^{-3}) is restricted to within 37 km of the coast, considerably narrower than upwelling regions off California and Baja.

The Pacific coast of South America, however, is subjected to the direct effects of the El Niño-Southern Oscillation (ENSO) cycle [e.g., see *Enfield,* 1989; and *Philander,* 1990], and local hydrographic [*Huyer et al.,* 1987, 1991] and biological [*Barber and Chavez,* 1983, 1986] patterns exhibit strong interannual variability. *Strub et al.* [1998] review El Niño conditions off the coast of South America, which include strengthening of poleward flow along the coast, deepening of the thermocline, shifting in the location of maximum upwelling favorable winds, and changing of the land-sea temperature gradient. These last two factors at least partially offset each other and result in the persistence of local upwelling favorable winds. Off Chile, satellite data show surface interannual variability is manifest as positive and negative sea surface temperature (SST) anomalies during the El Niño (warm) and La Niña (cold) phases of the cycle [*Yanez et al.,* 1995]. Additional nonseasonal variability and direct equatorial connections result from equatorial waves, which propagate into the region as coastal trapped waves [*Enfield et al.,* 1987; *Shaffer et al.,* 1997].

From 1996 to early 1998 the eastern Pacific progressed from relatively cold La Niña conditions to warm El Niño conditions [*Chavez et al.,* 1998]. In an accompanying paper, J.L. Blanco et al. (Hydrographic conditions off northern Chile during the 1996-1998 La Niña and El Niño, submitted to *Journal of Geophysical Research,* 2000, hereinafter referred

[1]School of Marine Sciences, University of Maine, Orono, Maine.
[2]Instituto de Fomento Pesquero, Valparaiso, Chile.
[3]Jet Propulsion Laboratory, Pasadena, California.
[4]College of Oceanic and Atmospheric Sciences, Oregon State University, Corvallis, Oregon.

Paper number 1999JC000052
0148-0227/01/1999JC000052$09.00

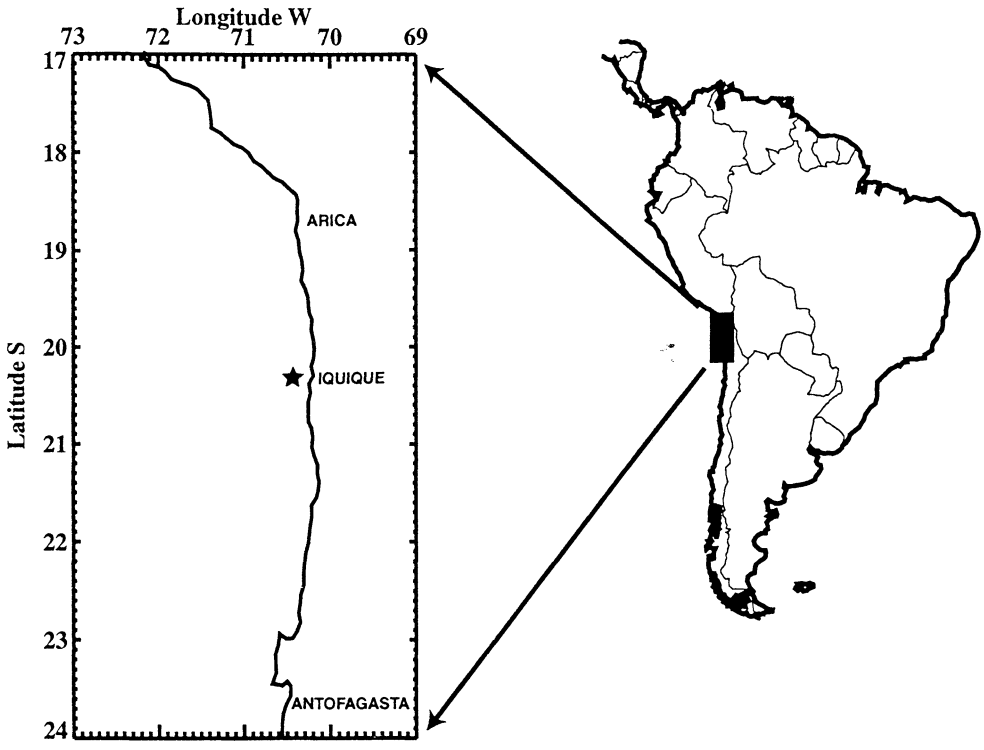

Figure 1. Map of the study area of northern Chile (18°–24°S) showing the region from 17° (southern Peru) to 24°S. The star indicates the location of the hydrographic monitoring station.

to as Blanco et al., submitted manuscript, 2000) present the temporal evolution of hydrographic conditions in the northern Chile coastal region over this ENSO cycle. The El Niño conditions of 1997-1998 include some of the strongest local hydrographic anomalies on record. Briefly, hydrographic conditions followed a normal [see *Blanco et al.* 2000] seasonal cycle in 1996 and up to March 1997 but with negative sea level and SST anomalies associated with the La Niña conditions. Beginning in March 1997, temperature and sea level anomalies became positive. Maximum anomalies occurred during two sea level peaks in May 1997 (austral fall) and in December 1997 (early austral summer) when surface flow was strongly poleward, disrupting the normal seasonal cycle. Strong positive surface anomalies continued until March 1998. By May 1998, SST had returned to near-climatological conditions. Readers are referred to Blanco et al. (submitted manuscript, 2000) for more details of the horizontal and vertical structure associated with this temporal evolution.

Satellite data allow a more detailed examination of the temporal and spatial evolution of patterns from the relatively cold regime present in 1996 through the arrival of El Niño conditions in 1997 and the recovery to near-climatological conditions by mid-1998. The launch of NASA's Sea-viewing Wide Field-of-view Sensor (SeaWiFS) mission in mid-1997 initiated operational measurements of mesoscale chlorophyll patterns in the global ocean. In this paper we present a general overview of biological responses to the hydrographic patterns presented by Blanco et al. (submitted manuscript, 2000). Patterns extracted from concurrent ocean color and SST satellite data of the upwelling region of northern Chile, coincident with the hydrographic data of Blanco et al. (submitted manuscript, 2000), are examined to show their coevolution in time. The imagery provides a more continuous examination of evolving patterns than that possible from cruise data and an estimation of the extent to which the annual cycle of cross-shelf patterns may have been affected by the El Niño. In section 2 we present the data, processing, data reduction, and analysis methodology. In section 3, time series of SST and SeaWiFS chlorophyll are presented both as images during specific periods and as more continuous time series of cross-shelf profiles. These are placed in temporal context using the evolution of vertical thermal structure measured at a hydrographic station. In section 4 comparisons of satellite-measured biological and physical variability, contrasting La Niña and El Niño periods, are provided. Concurrent wind and surface chlorophyll measurements are presented and compared to the satellite data time series. In section 5 we present a summary.

2. Data and Methods

The SeaWiFS mission began producing global images of ocean chlorophyll in September 1997. Daily level 2 global area coverage images of the South American Pacific coast were received from the Goddard Space Flight Center Distributed Active Archive Center and remapped to a standard projection covering the study area (Figure 1) at 4 km resolution. All scenes with valid data within the study region, beginning in September 1997, were used to form a time series of temporal composites over 8 day periods [*Campbell et al.*, 1995]. Chlorophyll retrievals are those of the second (1998) reprocessing. Full resolution National Oceanic and Atmospheric Administration (NOAA) advanced very high resolution radiometer (AVHRR) images are collected routinely at the Centro de Percepción Remota de la

Universidad Católica de Chile. All scenes of the study area from January 1996 to May 1998 were processed into images of SST using standard NOAA coefficients, multichannel algorithms, and cloud-screening techniques and then remapped to a standard projection at 1 km resolution. These data were formed into a time series of 7 day composites using all available passes. Composites with over 50% missing data over the study region were not included in the analysis. Differences are expected in the extent of cloud cover, and hence missing data, both seasonally and interannually. The extent to which this missing data might bias coverage by the AVHRR is unknown but is reduced by the formation of the temporal composites.

Surface temperature and chlorophyll patterns measured by the satellite data were extracted from each image in the time series as six cross-shelf profiles, spaced 1° of latitude apart over the latitudinal extent of the study area. Each cross-shelf profile was formed as a spatial mean of pixel values equidistant from the coast over a latitudinal range of 100 km centered at each of the six latitudes and progressing 200 km offshore, preserving the maximum spatial resolution of the satellite imagery in the cross-shelf direction.

Wind data are monthly means calculated from daily measurements made at the meteorological stations at the airports of Arica, Iquique, and Antofagasta. The measurements at 1500 hours were used, as these represent the maximum in both wind intensity and stability of direction and speed over the daily cycle. Climatological values used for comparison to study period conditions were calculated from a 27 year time series over the period 1970–1997 [*Blanco et al.* 2000]. The predominantly north-south orientation of the coast allows use of the v component to approximate alongshore wind.

3. Results

A time series of vertical temperature structure taken 10 km offshore at Iquique (20.5°S, see Figure 1) during ship surveys carried out by Instituto de Fomento Pesquero (IFOP) characterizes the temporal evolution of hydrographic conditions through the relatively cold period of 1996, the arrival of El Niño conditions in 1997, and recovery in 1998 (Plate 1). Detailed analysis of hydrographic conditions and anomalies associated with this period is given by Blanco et al. (submitted manuscript, 2000), and only a brief description will be given here to illustrate the timing of events and to place satellite-measured patterns into temporal context. The hydrographic time series (Plate 1) shows relatively weak vertical stratification (the 13°C isotherm is within the upper 110m) and cold surface anomalies during the period from late 1995 through early 1997. Cold surface anomalies are strongest in the (austral) summers of 1995-1996 and 1996-1997. Increased stratification and warmer surface water appear in the February-March period in 1997, similar to that of 1995, effectively ending the La Niña conditions. In May 1997, however, warm surface isotherms deepen rapidly with the arrival of the first El Niño pulse. The 13°C isotherm is deeper than 250 m, and positive anomalies > 2°C extend below 400 m. Surface anomalies remain > 4°C in July–August 1997 (winter). In the September–November period (austral winter–spring), isotherms shoal and anomalies weaken to 1°-2°C during a relaxation in El Niño conditions. A second pulse arrives with great rapidity in December 1997, pushing the 13°C isotherm below 300 m and creating positive anomalies > 3°C down to 250 m. This second pulse is both longer-lived and stronger than the first. Surface anomalies > 4°C are present through March 1998. Beginning subsurface in February 1998, however, El Niño conditions begin to weaken, and by May, ship data show that both surface and subsurface temperature conditions off northern Chile are approaching climatological means (Blanco et al., submitted manuscript, 2000).

Satellite SST patterns concurrent with the eight cruise periods presented by Blanco et al. (submitted manuscript, 2000) are shown as monthly composites in Plate 2. These provide a contrast between the spatial patterns during each season, affected by La Niña conditions in 1996 and El Niño conditions in 1997-1998. May 1996 through March 1997 represent an annual cycle from fall, through winter, spring, and summer. Coldest SST nearshore in each image indicates coastal upwelling of subsurface water, consistent with the climatological hydrographic fields associated with these seasons [*Blanco et al.* 2000]. Large-scale surface flow is equatorward throughout this period (Blanco et al., submitted manuscript, 2000). Mesoscale recirculation patterns in the southern portion of the study area in May 1996, evident in the geopotential anomaly fields and as negative anomalies in surface temperature and salinity in the cruise data (Blanco et al., submitted manuscript, 2000), appear as jets and eddies in the satellite imagery shown here. Negative temperature anomalies in the coastal upwelling zone in spring and summer (December 1996 and March 1997), especially off Iquique (21.5°S) (Blanco et al., submitted manuscript, 2000), indicate that the upwelling evident in the satellite imagery is stronger than normal. In May 1997, temperature and salinity surface anomalies switch to positive (Blanco et al., submitted manuscript, 2000), most strongly in the southern portion of the study area, and are associated with anomalous poleward surface flow. The satellite image for this period confirms this warming, with strongest differences between the 2 years evident in the south and along the coastal upwelling region. This overall SST difference between years, especially within the upwelling region, is present through winter, spring, and summer in the satellite data (August 1997, December 1997, and March 1998), coincident with the strongest surface temperature and salinity anomalies. Warm SST encroaches all the way to the coast during December 1997 and March 1998, largely eliminating the surface signature of upwelling along the coast.

Annual cycles of cross-shelf SST structure during the 1996–1998 study period are shown in Figure 2 at six locations spanning the study area. Data from 1996 (Figure 2a) illustrate temporal evolution of patterns during the relatively cold La Niña conditions. SST is highest (> 22°C) offshore (> 50 km) during austral summer (January–March) with a maximum in February. Within 50 km of shore, coastal upwelling [*Blanco et al.* 2000; Blanco et al., submitted manuscript, 2000] reduces SSTs and creates relatively strong cross-shelf gradients. Within 30 km of shore, SSTs are generally < 19°C. In April (fall), SSTs begin to drop over the entire 200 km wide sampled region, most strongly in offshore regions (> 50 km). By May most cross-shelf surface thermal structure is gone, and temperatures < 17°C dominate the region from 0 to 200 km offshore throughout winter. Beginning in October (austral spring) at the lowest latitudes and November at the

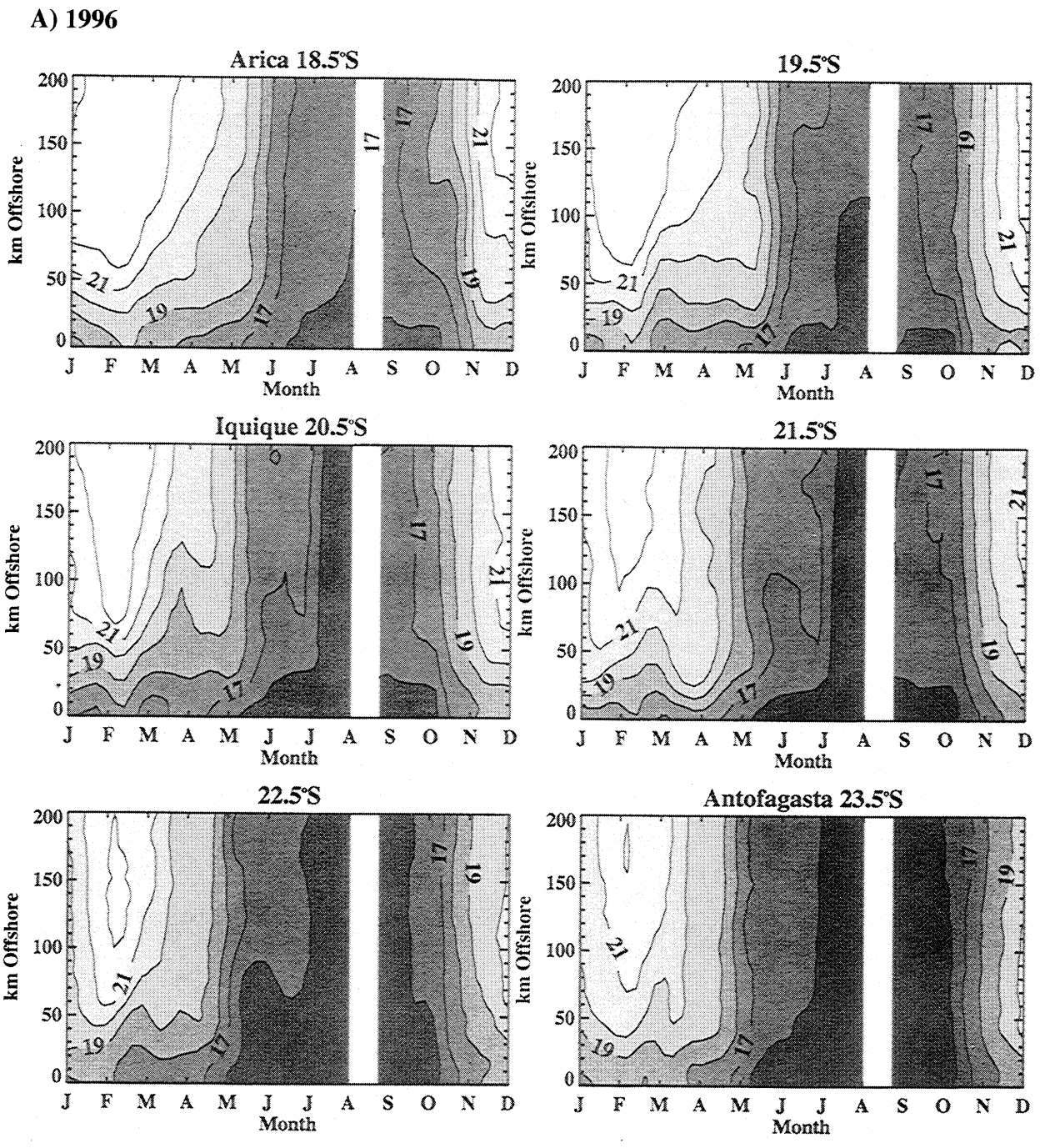

Figure 2. The seasonal distribution of SST (°C) off northern Chile in (a) 1996, (b) 1997, and (c) the first 5 months of 1998, plotted as contours in time and cross-shelf distance at six latitudes spanning the study area. Data are cross-shelf transects subset from the time series of 7 day composite NOAA AVHRR data. Each cross-shelf transect is a mean over 100 km in latitude, centered at each latitude.

higher latitudes, offshore temperatures increase, and by November–December, summer conditions are reestablished. Latitudinal variability within the study area is present, but variability in the cross-shelf direction is stronger. Lower latitudes experience longer summer periods of warm offshore water and shorter winter periods of cooler offshore water than higher latitudes. Colder coastal SST at Iquique (20.5°S), a known upwelling center, is evident. Despite the cold anomalies of this period (Plate 1) (Blanco et al., submitted manuscript, 2000) the annual cycle presented here is very similar to the normal cycle for the northern Chile upwelling region shown by *Barbieri et al.* [1995] and the climatology of *Blanco et al.* [2000]. The SST patterns of austral summer–early fall (January–April) 1997 (Figure 2b) are similar to those of 1996, with strong cross-shelf gradients within the first 50 km, temperatures < 19°C within 25 km of shore, and temperatures > 22°C offshore. After April, however, distinct differences become apparent. Warm offshore conditions persist longer into the austral fall-winter period than they did in 1996. Winter (July-September) temperatures are warmer,

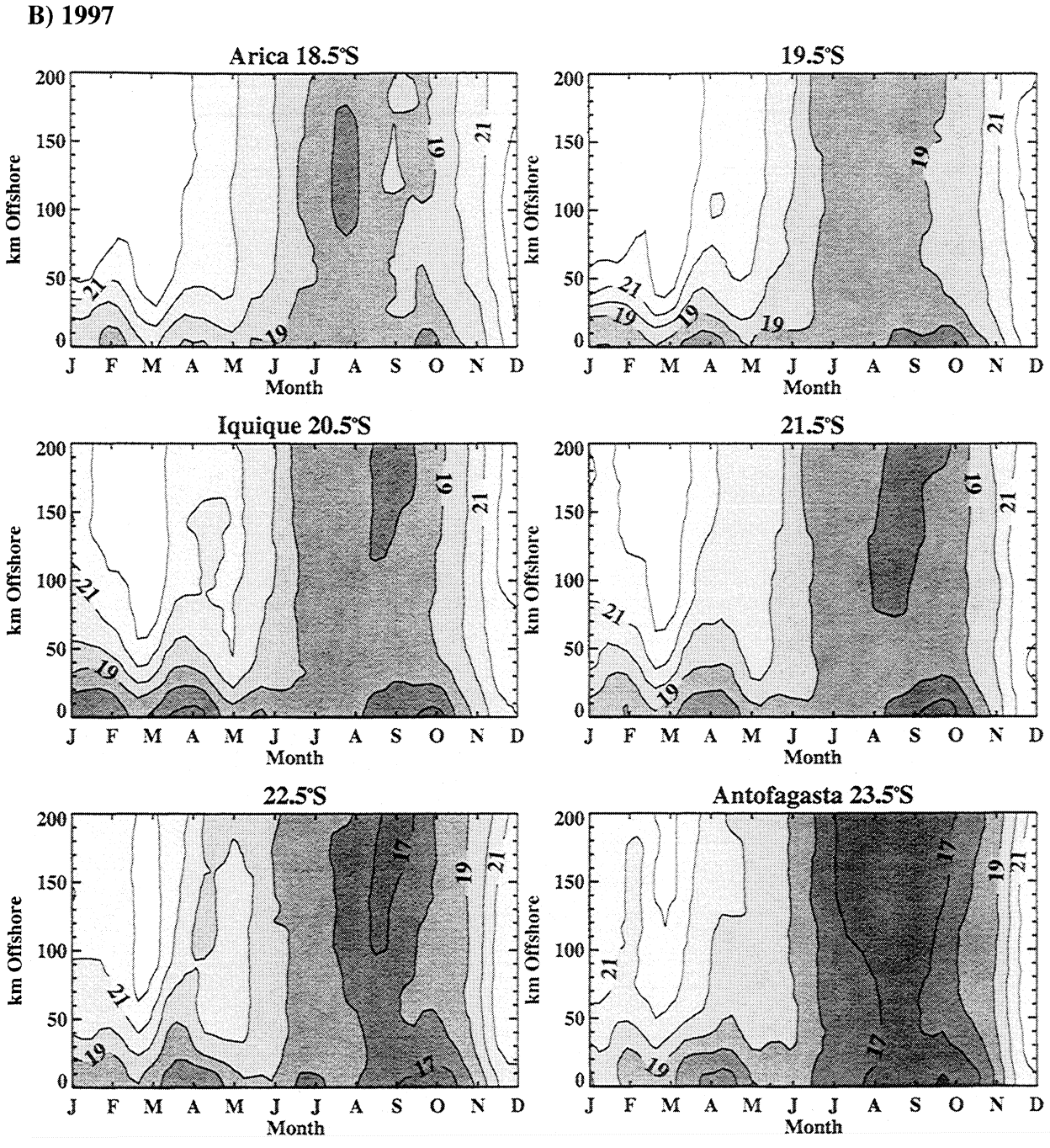

Figure 2. (continued)

decreasing below 17°C only at the two highest latitude transects. Warming in spring (November–December) is stronger than was observed in 1996, and warm offshore temperatures (21°C) intrude all the way to the coast, resulting in very little cross-shelf thermal structure. This trend is carried through to early 1998 (Figure 2c), where summer (January–February) cross-shelf patterns are dramatically different from those in both early 1996 and early 1997. Temperatures are > 21°C adjacent to the coast, and the entire offshore region from 25 to 200 km is dominated by SST > 22°C. Beginning in March, however, cooler SST is observed within 25 km of shore, and in April, SST begins to decrease in the offshore regions. By May 1998, cross-shelf SST patterns resemble those of May 1996.

SeaWiFS data first became available in September 1997, during the relaxation period between the two major El Niño pulses (Plate 1). This provides four chlorophyll images coincident with hydrographic fields discussed by Blanco et al. (submitted manuscript, 2000). These are presented in Plate 3 as a sequence of monthly composites (using September 1997 to represent the August 1997 (spring) cruise period). Each image shows elevated chlorophyll concentrations in the upwelling region nearshore and lower concentrations offshore. In September (winter), chlorophyll concentrations in

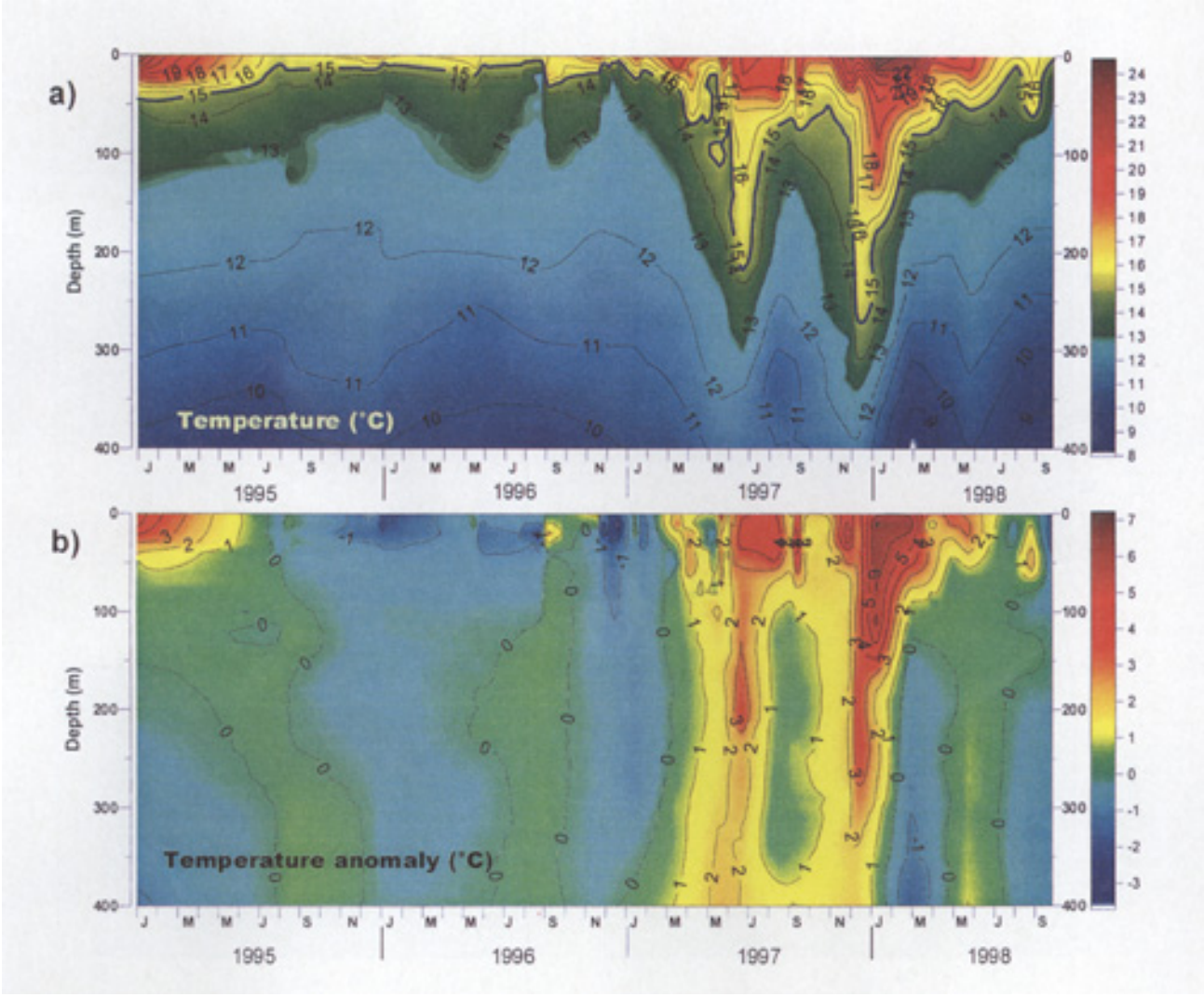

Plate 1. Time series of (a) vertical temperature structure and (b) temperature anomalies from January 1995 to May 1998 measured 10 km offshore at 20.5°S during approximately monthly cruises. Anomalies are from a 30 year climatology at the same location, discussed in detail by *Blanco et al.* [2000].

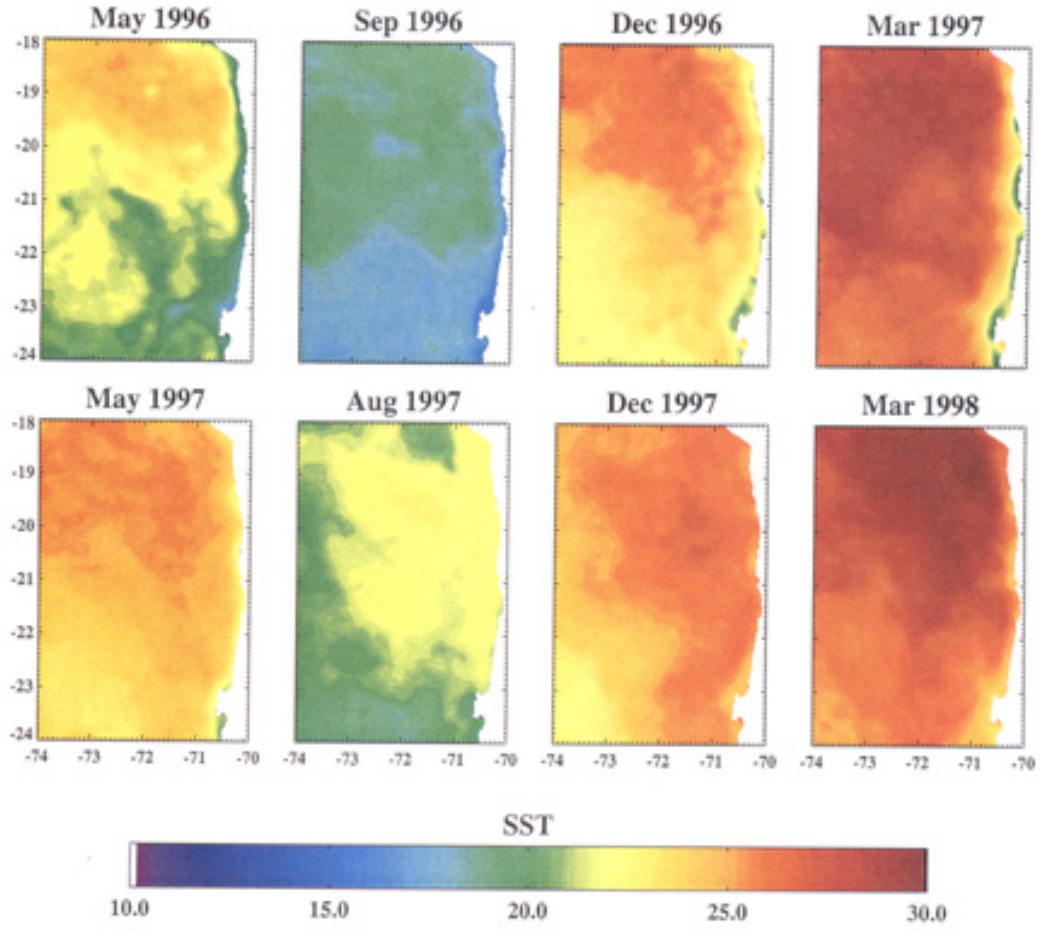

Plate 2. Monthly composites of satellite SST (°C) for the study region, representative of austral fall (May), winter (September and August), spring (December), and summer (March) conditions during La Niña (1996) and El Niño (1997-1998). Months correspond to the hydrographic fields presented by Blanco et al. (submitted manuscript, 2000).

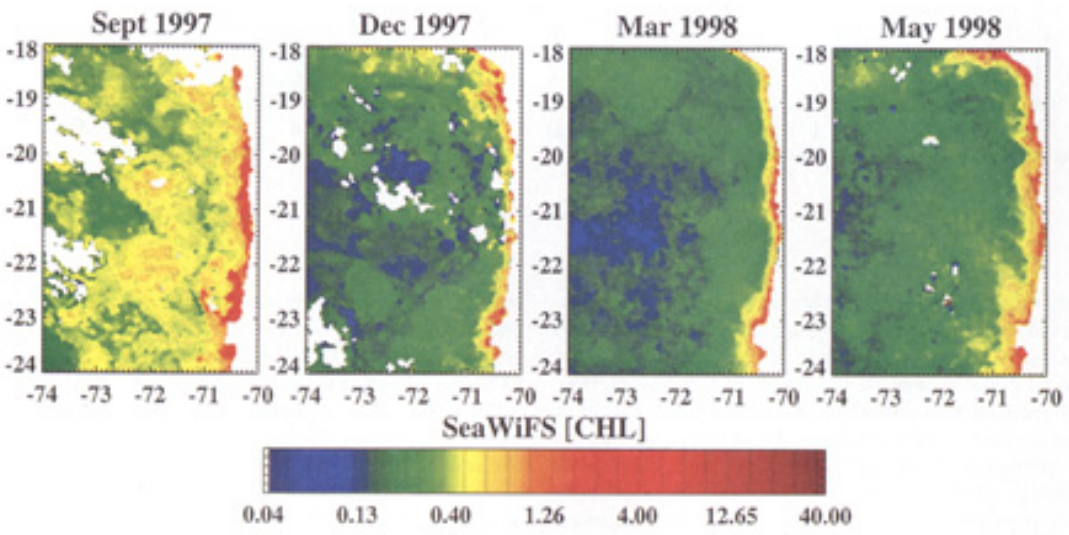

Plate 3. Monthly composites of SeaWiFS chlorophyll concentration (mg m^{-3}) for the study region, representative of winter (September), spring (December), summer (March), and fall (May) conditions during El Niño (1997-1998). Months correspond to hydrographic fields presented by Blanco et al. (submitted manuscript, 2000), beginning with the start of the SeaWiFS mission.

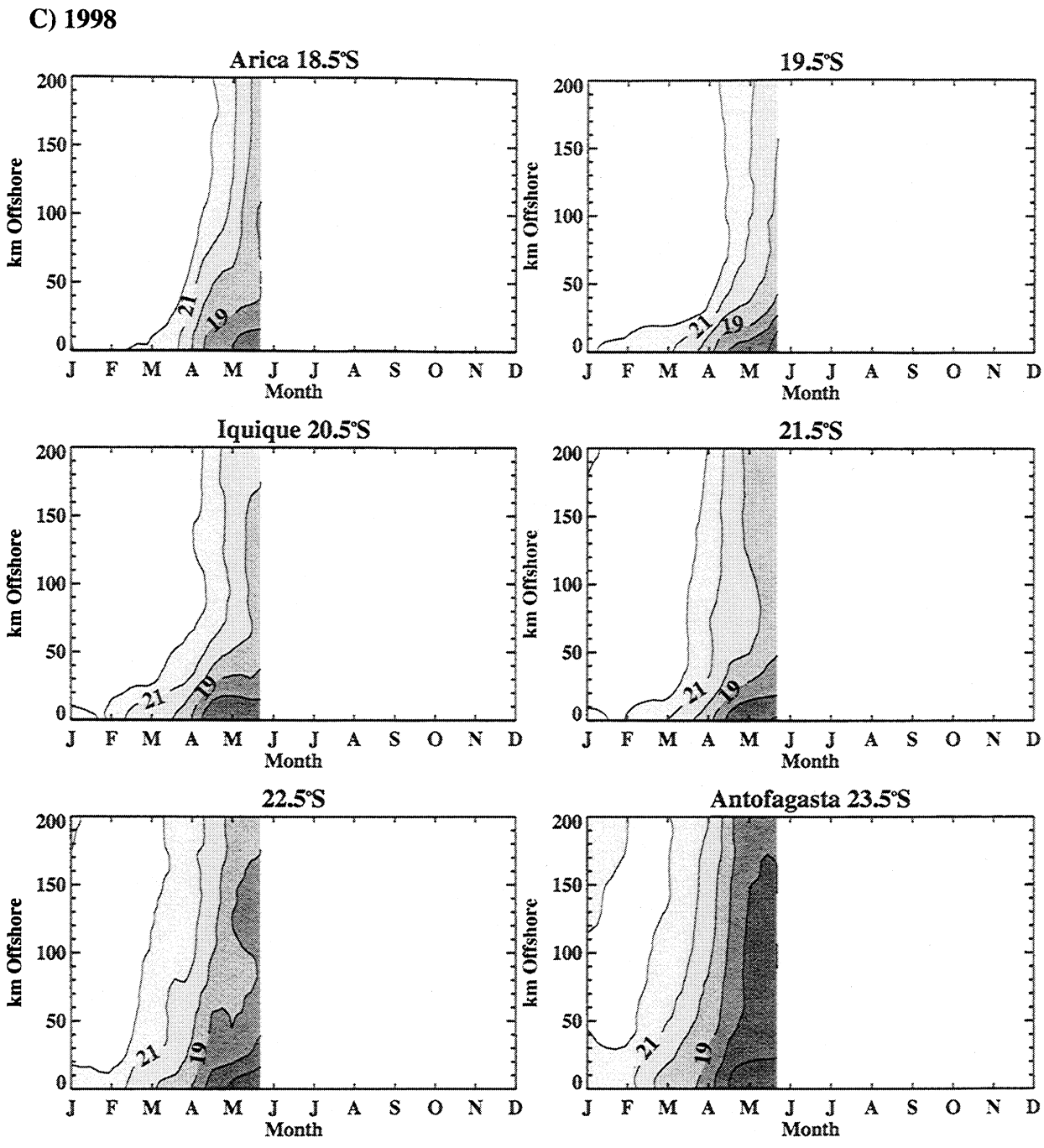

Figure 2. (continued)

the offshore zone (west of 71°W) are the highest (> 0.5 mg m^{-3}) observed over the study period, apparently associated with eddy-like structures. In December, at the time of maximum positive El Niño anomalies and anomalous poleward flow these offshore concentrations drop to < 0.3 mg m^{-3}, except in the most northerly region, evidence of offshore eddy structure largely disappears, and both the width and chlorophyll concentration of the coastal zone decreases. These offshore and coastal trends continue into March 1998 when surface thermal anomalies have begun to subside but salinity anomalies are still strong (Blanco et al., submitted manuscript, 2000). In May 1998 (fall), offshore concentrations remain relatively low, but inshore of 71°W both the width and concentration of coastal chlorophyll are greater than those of December and March throughout the latitudinal range of the study area.

The temporal evolution of cross-shelf chlorophyll concentrations from the beginning of the SeaWiFS mission to the end of May 1998 is shown in Figure 3. In general, elevated chlorophyll concentrations within 50 km of the coast and more oligotrophic conditions offshore are evident throughout the study area. In early September, 1.0 mg m^{-3} is the maximum chlorophyll concentration present and is restricted to within 15 km of shore. Later in September and

through October, nearshore concentrations increase to > 2.0 mg m^{-3}, and concentrations > 1.0 mg m^{-3} expand offshore to distances of 30-50 km. Both concentrations and cross-shelf extension of elevated concentration collapse during November at all latitudes except the most northerly (18.5°S). By December, maximum concentrations within 10 km of the coast are 0.5 mg m^{-3}, except at the two lowest latitudes, where concentrations > 1.0 mg m^{-3} remain. Oligotrophic offshore water (< 0.25 mg m^{-3}) is present within 50 km of the coast beginning in January 1998 and maintains this pattern until March. Offshore concentrations begin to increase in March (> 0.25 mg m^{-3}) at the three higher latitudes, while nearshore (< 10 km) concentrations surpass 1.0 mg m^{-3} and all latitudes show the 0.5 mg m^{-3} isoline expanding offshore. In April, there is an increase in concentrations near the coast at all latitudes to > 1.0 mg m^{-3} and concentrations up to 0.5 mg m^{-3} extend offshore to distances of 40-60 km. In May at the lowest latitude studied (18.5°S), concentrations > 0.5 mg m^{-3} extend 150 km offshore, similar to those of early September 1997.

4. Discussion

4.1. Comparisons of Temperature and Chlorophyll Patterns

Earlier work with Coastal Zone Color Scanner (CZCS) imagery illustrates the value of concurrent SST and ocean color satellite imagery in understanding evolving biological–physical patterns. *Arnone and LaViolette* [1986] show a close relationship between thermal and color features in eddies along the North African coast. Within eastern boundary currents the relationship between satellite-measured cold

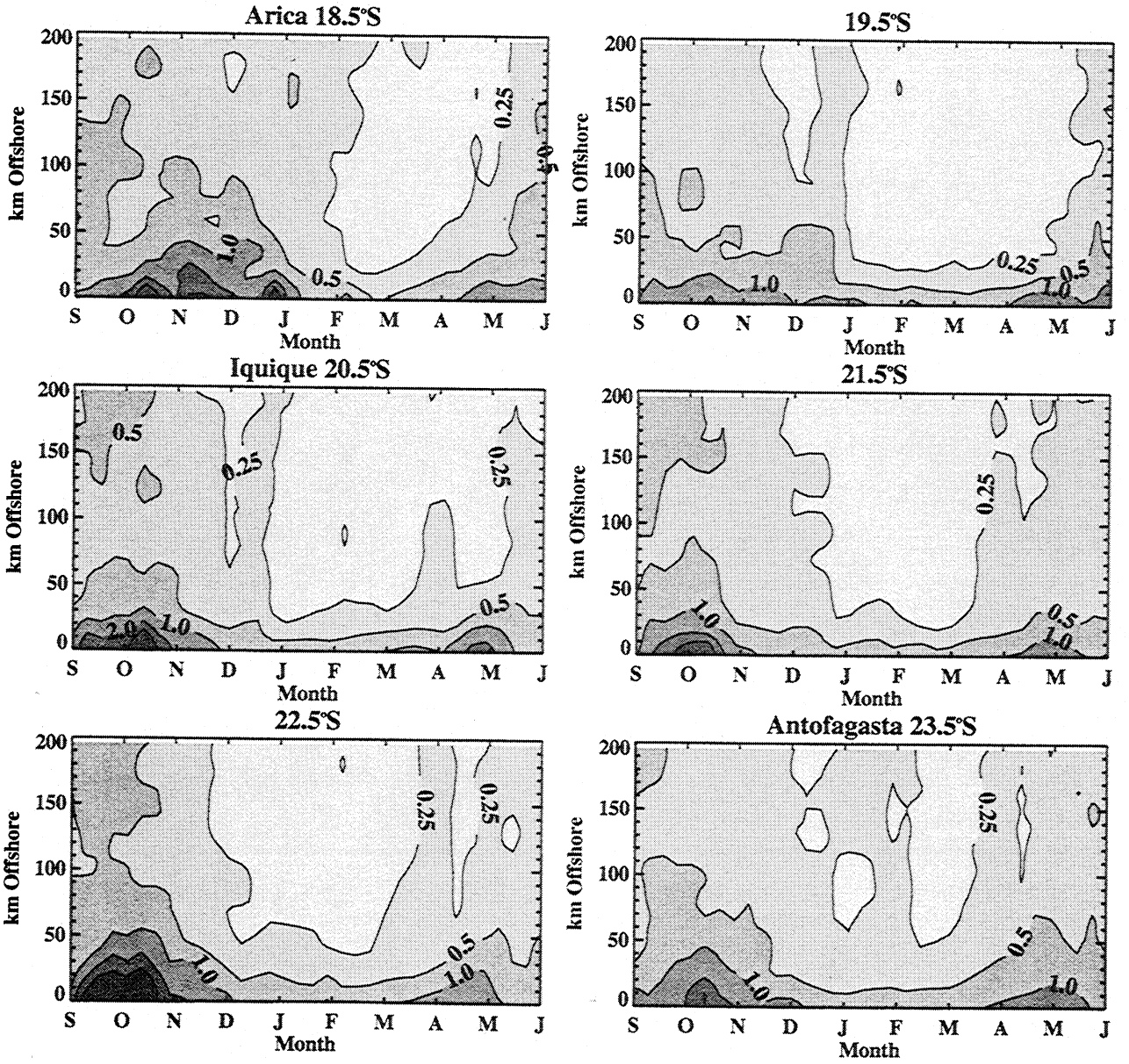

Figure 3. The temporal evolution of satellite-measured cross-shelf chlorophyll concentration (mg m^{-3}) off northern Chile in 1997–1998 at the six latitudes used in Plate 2. Cross-shelf transects are subset from the time series of 8 day SeaWiFS composite images at 4 km resolution and are a latitudinal mean over 100 km at each location.

upwelled water and pigment concentrations is well documented [e.g., *Abbott and Zion,* 1985; *Van Camp et al.,* 1991]. Here we examine the relationship between the temporal evolution of SST and chlorophyll patterns with two approaches; first, using the strength and position of surface thermal fronts and, second, using an index of coastal upwelling intensity.

Previous work in the California Current [*Strub et al.*, 1991; *Hood et al.*, 1991] has shown that elevated pigment concentrations resulting from coastal upwelling are found on the inshore side of the main current jet and hydrographic frontal zone. Cross-shelf extensions of higher chlorophyll concentrations characteristic of the upwelling zone are thus modulated by the cross-shelf position of the jet and frontal zone. If similar biological-physical dynamics operate within the northern Chilean upwelling system, we would expect cross-shelf patterns of chlorophyll to be associated with the position and strength of the frontal zone, which we can characterize in the satellite data by the SST spatial gradient. The time series of 7 day composite SST images were transformed into SST gradient images, defined at each spatial point as the unweighted two-dimensional gradient magnitude given by $|T(x,y)| = 1/(2\Delta h)\{[T(x-\Delta h,y) - T(x+\Delta h,y)]^2 + [T(x,y-\Delta h) - T(x,y+\Delta h)]^2\}^{1/2}$, where T is the temperature at a particular x,y location and h is a horizontal separation. Cross-shelf transects were then subsampled from these gradient images at the six latitudes used in Figures 2 and 3. Cross-shelf SST gradient structure evident in these six transects (and in Figure 2) indicated that while latitudinal variability is present, similar temporal patterns exist at each of the six latitudes. For brevity the six transects were averaged together to form a single cross-shelf gradient pattern for each time period (weekly composite), representative of the mean over the latitudinal range of the study area. Figure 4 shows the annual cycle of SST frontal strength, contoured as a function of time and cross-shelf position, over the 1996-1998 study period. The time series for 1996-early 1997 (Figures 4a and 4b) shows patterns during La Niña conditions and establishes the seasonal cycle during a non-El Niño year. Fronts within the study area are strongest and have the largest cross-shelf extension in austral summer–early fall (January-April). In May, fronts stronger the 0.05°C km^{-1} disappear, and weaker fronts are closer inshore. In late austral fall-winter (June–September), SST fronts are minimum, and those present are relatively close to shore (within 60 km). Beginning in spring (October), frontal position begins to shift farther offshore. This continues to increase through December-January, when fronts stronger than 0.05 °C km^{-1} are again present within 50 km of shore and weaker fronts extend 200 km offshore. SST frontal patterns in the early portion of 1997 (Figure 4b) are similar to that of 1996, with maxima in both strength and cross-shelf position in summer–early fall (January–April), although fronts in early fall (April) do not extend as far offshore. Thereafter, in 1997, however, distinct differences are apparent. Gradients weaken and are present closer to shore in late fall–winter (June), earlier in the year than those of 1997 and much weaker nearshore (gradients > 0.03°C km^{-1} are not present). They become stronger and are farther offshore in September–early October but then weaken again and are closer to shore in spring (November–December). In 1998 (Figure 4c) the relatively weak gradients are still present in January. In February, fronts strengthen and begin to progress offshore, such that by April-May, patterns in 1998 resemble those of 1996 and 1997. These gradient data suggest that the strong SST anomalies associated with the May 1997 pulse (Plates 1 and 2b) occurred at a time when the normal seasonal pattern of frontal activity is weakening and shifting inshore. Differences between winter (July–September) 1997 and 1996 are not obvious. The second pulse, however (December 1997, Plate 1), occurs in late spring-early summer, when gradients during non-El Niño conditions (1996) are maximum in both magnitude and cross-shelf extension, creating strong differences between the 2 years. These differences are carried through the summer into 1998 (January–March) with weaker gradients located closer to shore than those present in early 1997.

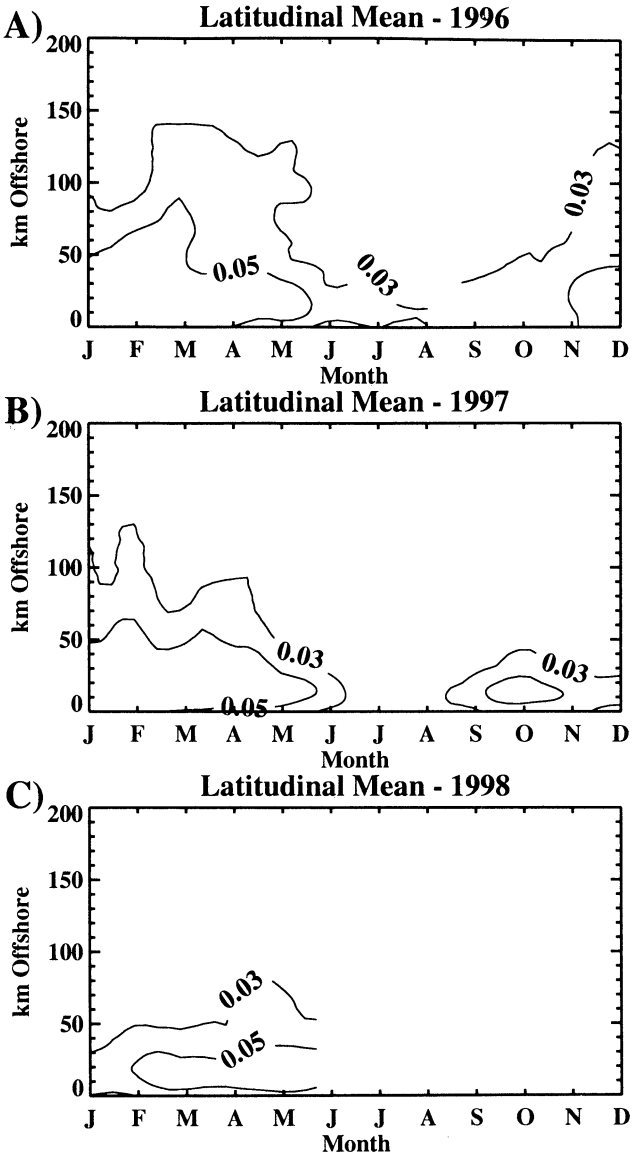

Figure 4. Seasonal cycles of frontal strength and position calculated as the two-dimensional gradient magnitude of SST in (a) 1996, (b) 1997, and (c) the first 5 months of 1998. Values are means over the latitudinal extent of the study area plotted as contours in time and cross-shelf distance. Data are calculated from time series of 7 day NOAA AVHRR composite images.

Comparisons with the chlorophyll patterns in Figure 3 show that the elevated chlorophyll concentrations that

develop in late September-October 1997 are associated with the brief strengthening of SST gradients (Figure 4b) and increasing cross-shelf extension that occurred in the relaxation period between the major El Niño pulses (Plate 1). This is consistent with the conceptual model that upwelling produces strengthened frontal gradients and increased nutrient availability, leading to higher coastal phytoplankton biomass. Relatively low coastal concentrations and reduced offshore extension of chlorophyll in November 1997-February 1998 are associated with weak gradients restricted to the nearshore region at the time of, and immediately following, the arrival of the second pulse of strong anomalies (Plate 1). Data from 1996 suggest that SST (Figure 2 and Plate 3) and frontal structure (Figure 4) during this El Niño period are dramatically different than normal austral summer conditions. In fall (April–May) 1998, chlorophyll concentrations increase nearshore and expand in a cross-shelf direction in association with the strengthening and offshore migration of SST fronts.

Comparisons between SST fronts and chlorophyll time/space patterns are simplified by decomposing the variance associated with each using empirical orthogonal functions (EOFs). The cross-shelf transect of both chlorophyll and gradient magnitude at 20.5°S is presented as an example; other profiles had similar variance structure. The dominant mode of chlorophyll variability (Figure 5a) explains 81% of the variance and captures the El Niño signal. The spatial pattern associated with this mode shows a simple cross-shelf gradient with maximum concentrations restricted to within 20 km of shore. The amplitude of this pattern is strongest in September-October, with a peak in early October, becomes weak from mid-November until March, and then strengthens to a peak in late April. The EOF decomposition of the gradient magnitude time series coincident with the chlorophyll time series is shown in Figure 5b. The dominant mode explains 82% of the variance, with a spatial pattern showing maximum gradients located 20 km offshore, spatially coincident with the offshore edge of elevated chlorophyll concentrations. The amplitude time series indicates this pattern increases to intermediate strength in late October, is weakest in December (coincident with the arrival of the second peak of SST anomalies (Plate 1)) and then becomes strong again in March and late April, showing many similarities to the chlorophyll amplitude time series. These data suggest control of cross-shelf pigment structure by the SST frontal zone and any current jet associated with it, consistent with observations in the California Current during the coastal transition zone experiment [*Strub et al.*, 1991]. Although SeaWiFS data are not available from the 1996 period for comparison, EOF analysis of the gradient magnitude time series for 1996 (Figure 5c) provides a contrast of the frontal patterns between El Niño and La Niña years. This contrast can be used to imply differences that might be expected in chlorophyll pattern during 1996. Months from 1996 have been rearranged to emulate the monthly sequence coincident with the availability of SeaWiFS data from 1997 to 1998 for direct comparison. The dominant mode (Figure 5c) explains 57% of the variance, considerably less than that of the 1997-1998 series, indicating more complex space/time patterns and increased variance associated with frontal patterns spread across higher modes. The spatial pattern in this La Niña year shows significant differences from that of 1997-1998. Strong fronts extend farther offshore, out to ~75 km. The total cross-shelf width of increased frontal activity is stretched over ~50 km, wider than that evident in 1997-1998, with two distinct peaks located 25 and 60 km offshore. The amplitude time series also shows a very different seasonal cycle than that of 1997-1998. The pattern is weak in September-October (late winter–early spring), a time when the 1997-1998 time series indicated a local maximum. In 1996 the pattern strengthens in November to a peak in early February (midsummer), times when the pattern in 1997-1998 was weakest. In late summer (March) the pattern weakens to a

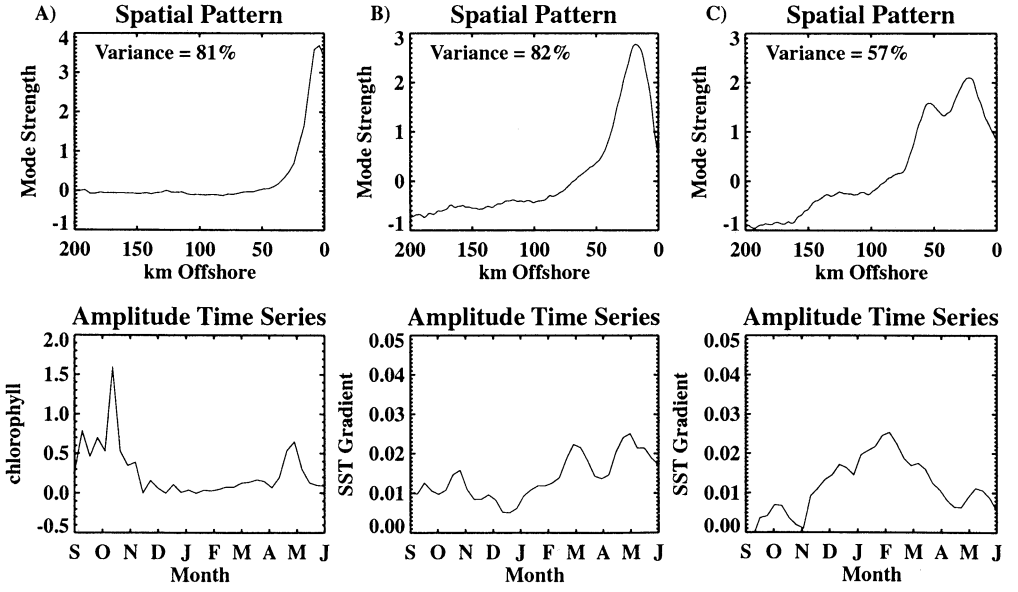

Figure 5. EOF decompositions of (a) cross-shelf SeaWiFS chlorophyll distributions over the 1997–1998 study period, (b) cross-shelf SST gradient magnitude for the same period, and (c) cross-shelf SST gradient magnitude for 1996, prior to El Niño conditions. The largest mode and its associated variance are presented in each case, showing both the spatial pattern and an amplitude time series. Months in 1996 (Figure 5c) were rearranged into the same order as the SeaWiFS data period to facilitate comparison.

local minimum in mid-April, opposite to that associated with the El Niño conditions of 1997-1998. The amplitude time series for 1996 is consistent with frontal activity expected from the climatological annual cycle of upwelling favorable wind forcing presented by *Blanco et al.* [2000].

Elevated coastal chlorophyll concentrations in eastern boundary currents result from the upwelling of cold, nutrient-rich water, and time series of nearshore SST measurements should contain any seasonal signal of upwelling intensity. The upwelling signal, however, is superimposed on, among other factors, both the annual cycle of surface solar heating, which at the latitudes examined here is considerable, and any horizontal advective processes influencing SST. For this reason the seasonal cycle of upwelling strength (cold water near the coast) is poorly captured in a simple time sequence of coastal SST. A partial correction can be made for these effects by assuming that the annual cycle of solar heating is the same at offshore locations of equal latitude and that surface advective processes influencing SST are small relative to the annual cycle and differences caused by upwelling. An index of coastal upwelling, which we call the "coastal SST deficit" [*Hill et al.*, 1998; *Thomas*, 1999], is formed by subtracting the coastal SST (the 1 km nearest shore) in each time period from the SST 200 km offshore at the same latitude. This coastal deficit captures a large-scale one-dimensional (cross-shelf) aspect of the gradient structure presented above as a localized small-scale two-dimensional calculation in Figure 4. A mean coastal deficit over the study region for each time period was formed by averaging in latitude. The annual cycle over the 14 month period beginning in January 1996 and in January 1997 is shown in Figures 6a and 6b to contrast upwelling signals in the La Niña and El Niño conditions, respectively. In 1996–early 1997 the coastal deficit is maximum (> 4 °C) in summer (January–February), indicative of relatively cold coastal SST, when annual maxima in both upwelling wind forcing and solar heating produce maximum differences between the coast and offshore waters [*Blanco et al.* 2000]. Deficit decreases steadily to a minimum (1°C) in winter (August) and then rises again. In 1997-early 1998 the annual cycle begins similarly in summer (January–March) 1997 but decreases more rapidly in May to a prolonged and lower (< 1 °C) minimum from early July through late September. There is a brief recovery period in spring when the deficit increases, but in late spring and summer the deficit decreases again to a second minimum in December-January, coincident with the maximum El Niño anomalies (Plate 1). The 1997-1998 time series is resampled over the time period of coincident SeaWiFS data (Figure 6c) to facilitate direct comparison to chlorophyll patterns (Figure 3). The data show that maximum coastal deficits did not develop until late in the study period (April–May 1998). In September the deficit is initially low, as is coastal chlorophyll concentration. The short-lived deficit increase in late October–November during the relaxation period between the large temperature anomalies is coincident with the spring increase in chlorophyll concentration (Figure 3). In December the coastal deficit drops to near zero, coincident with the arrival of the second El Niño pulse and very low coastal chlorophyll concentrations. The low coastal deficit through the austral summer and the subsequent increase toward the May maximum are positively correlated with the chlorophyll patterns. For comparison, the coastal deficit over the same monthly sequence during La Niña conditions is shown in Figure 6d, highlighting significant differences between the two phases of the ENSO cycle. Assuming a similar linkage between deficit and chlorophyll as that shown in Figures 3 and 6 for 1997-1998, the deficit time series from 1996 implies a very different annual chlorophyll pattern, with maximum coastal concentrations in summer, coincident with maximum seasonal wind forcing and minimum concentrations and cross-shelf structure in winter. Such a

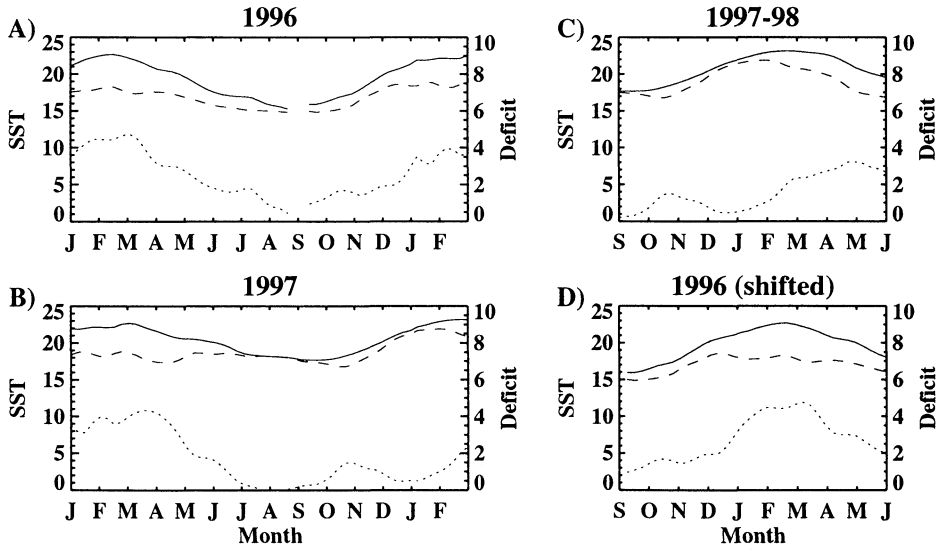

Figure 6. Coastal SST deficit (dotted line) calculated as the difference between coastal SST (dashed line) and SST 200 km offshore (solid line) (°C) in the 7 day composite SST image time series. The 14 month periods beginning in (a) January 1996 and (b) January 1997 contrast the annual cycle of coastal upwelling during La Niña and El Niño conditions respectively. The monthly sequence when SeaWiFS chlorophyll data are available are replotted for comparison to Figure 3 as both (c) the coincident 1997-1998 period and (d) the same months from 1996 with months rearranged to facilitate direct comparison. Values for each time period represent a latitudinal mean over the study area.

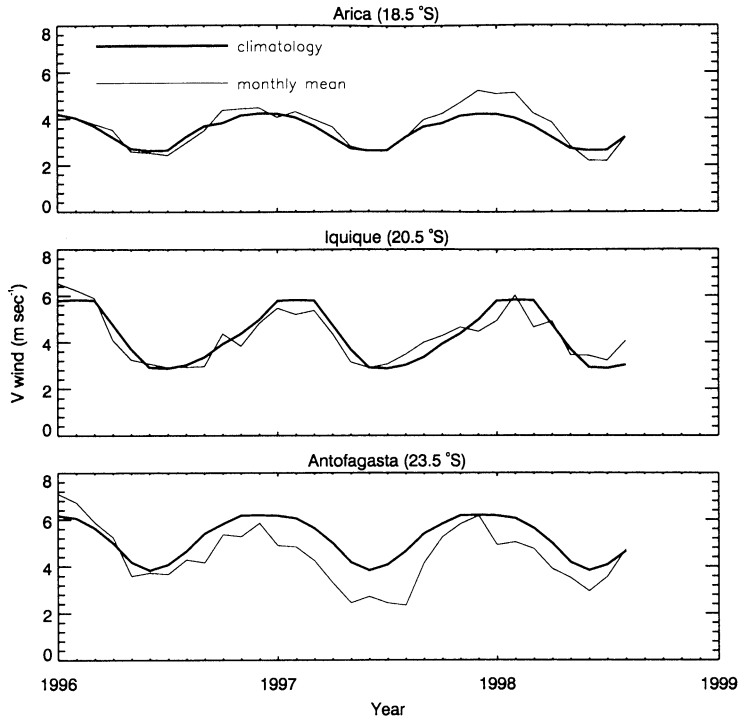

Figure 7. The *v* (alongshore) component of wind velocity (positive north) off northern Chile for 1996, 1997, and 1998 at three coastal meteorological stations (thin line) at Arica (18.5°S), Iquique (20.5°S), and Antofagasta (23.5°S). For comparison, the 10 year climatology [Blanco et al. 2000] of these stations is presented (bold line).

pattern would be consistent with the two seasons of field measurements presented by *Morales et al.* [1996].

4.2. Wind Forcing

The year-round coastal upwelling of northern Chile results from seasonally persistent equatorward (upwelling favorable) alongshore wind stress [*Blanco et al.* 2000]. Relaxations (or reversals) in local alongshore wind stress would result in warmer coastal surface temperatures and reduced phytoplankton biomass. Previous analyses of El Niño conditions in both the California and Peru-Chile upwelling systems have shown that wind stress is often not reduced during El Niño events or that local wind anomalies develop after the onset of El Niño conditions [*Huyer and Smith,* 1985; *Reinecker and Mooers,* 1986]. Under these situations, local offshore Ekman transport driven by continuing equatorward wind stress simply upwells anomalously warm and nutrient-poor subsurface water from above the strongly depressed pycnocline. Hydrographic patterns during the 1997-1998 El Niño are consistent with these previous observations (Blanco et al., submitted manuscript, 2000). Wind forcing along the northern Chile coast at Arica (18.5°S), Iquique (20.5°S), and Antofagasta (23.5°S) is shown in Figure 7 as alongshore wind velocity over the study period and climatological (1970-1997) monthly means available from [*Blanco et al.* 2000]. Discussion of wind anomalies and their relative timing during the 1997-1998 El Niño period are presented by Blanco et al. (submitted manuscript, 2000) and will not be repeated here. The important point, however, is that wind stress throughout the region remains equatorward over the entire study period. Upwelling of subsurface water and offshore transport, although diminished at the southern portion of the study region, was unabated and (in the north) even increased during the 1997-1998 period. These data indicate that surface temperature and chlorophyll patterns during the 1997-1998 El Niño period are not due to cessation of upwelling, a view consistent with the hydrographic analysis of Blanco et al., (submitted manuscript, 2000).

4.3. Comparisons to Other Satellite Chlorophyll Data

Available satellite pigment data from northern Chile from 1979 [*Thomas,* 1999], the only year during the CZCS mission with observations in enough months to attempt forming a seasonal cycle, provide additional comparison. Although CZCS pigment concentrations are lower (0.5–1.0 mg m^{-3} in the coastal region) than those of SeaWiFS, cross-shelf distances of maximum concentrations are similar, restricted to within 30 km. However, the CZCS annual cycle in 1979 suggests a late fall-winter maximum in concentrations (April–July), although both January and December have no data. This is out of phase with the SeaWiFS data from the El Niño period. This inconsistency may be due to inaccuracies in the actual CZCS pigment concentrations [*Chavez* 1995] but is also likely to be due to inadequate sampling by the CZCS in both time and space [*Thomas et al.*, 1994; *Thomas,* 1999].

Although SeaWiFS chlorophyll measurements are not available for the 1996 cold phase of the ENSO cycle captured by the AVHRR, chlorophyll data from the Ocean Color and Temperature Sensor (OCTS) aboard the ADEOS satellite are available as global monthly composites at 9 km spatial resolution for the period November 1996–June 1997 (the lifetime of the mission). Differences in the characteristics of the OCTS and SeaWiFS sensors make their respective chlorophyll concentration retrievals difficult to compare;

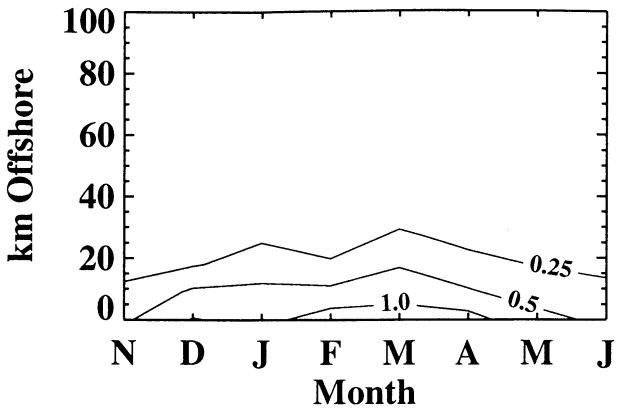

Figure 8. The distribution of OCTS satellite-measured chlorophyll (mg m^{-3}) off northern Chile from November 1996 to June 1997 plotted as contours in time and cross-shelf distance. OCTS data are from monthly composite images with 9 km spatial resolution. Cross-shelf values are averaged over the latitudinal extent of the study area in each month.

however, valid comparisons can be made of patterns in time and space. The 8 months of OCTS data were acquired, subset to the study area and the cross-shelf chlorophyll distribution, averaged over the latitudinal extent of the study area, calculated in each month. The 9 km resolution OCTS data do not resolve the upwelling region and gradients as well as the 4 km SeaWiFS data, but the time series of the cross-shelf chlorophyll concentrations (Figure 8) provide a clear indication of trends over the period. Both cross-shelf extension and nearshore values of elevated chlorophyll concentrations are minimum in November 1996 (spring) and increase to a maximum in austral summer and early fall (February–April). Thereafter both decrease until June (winter) 1997 when patterns are similar to those of November 1996. The summer maximum evident in these data is clearly different from patterns in 1997-1998 (Figure 3). The 1996-1997 summer maximum is consistent, however, with the climatological seasonal maximum in upwelling favorable wind forcing [*Blanco et al.*, 2000] as well as both the AVHRR-measured frontal strengths (Figures 4a, 4b and 5c) and the temporal pattern of SST deficit (Figure 6d) for 1996.

A second indication of the extent to which the 1997-1998 seasonal chlorophyll patterns are disrupted by El Niño conditions can be obtained by examining SeaWiFS data from the following year (1998-1999). Cross-shelf profiles from the period September 1998 to March 1999 (Figure 9) show maximum chlorophyll concentrations in midsummer (January-February), in phase with the maximum in climatological wind forcing (*Blanco et al.* 2000) and consistent with the summer seasonal maximum of nearshore phytoplankton pigment observed in the California Current in CZCS data [*Strub et al.*, 1990; *Thomas and Strub*, 1990]. Contrasts between the SeaWiFS spatial patterns evident in September and December of both years are consistent with those reported by *Morales et al.* [1996]. Maximum concentrations are restricted to within 30-40 km of shore, and elevated concentrations extend farther offshore, resulting in a reduced cross-shelf gradient in late winter (September). The

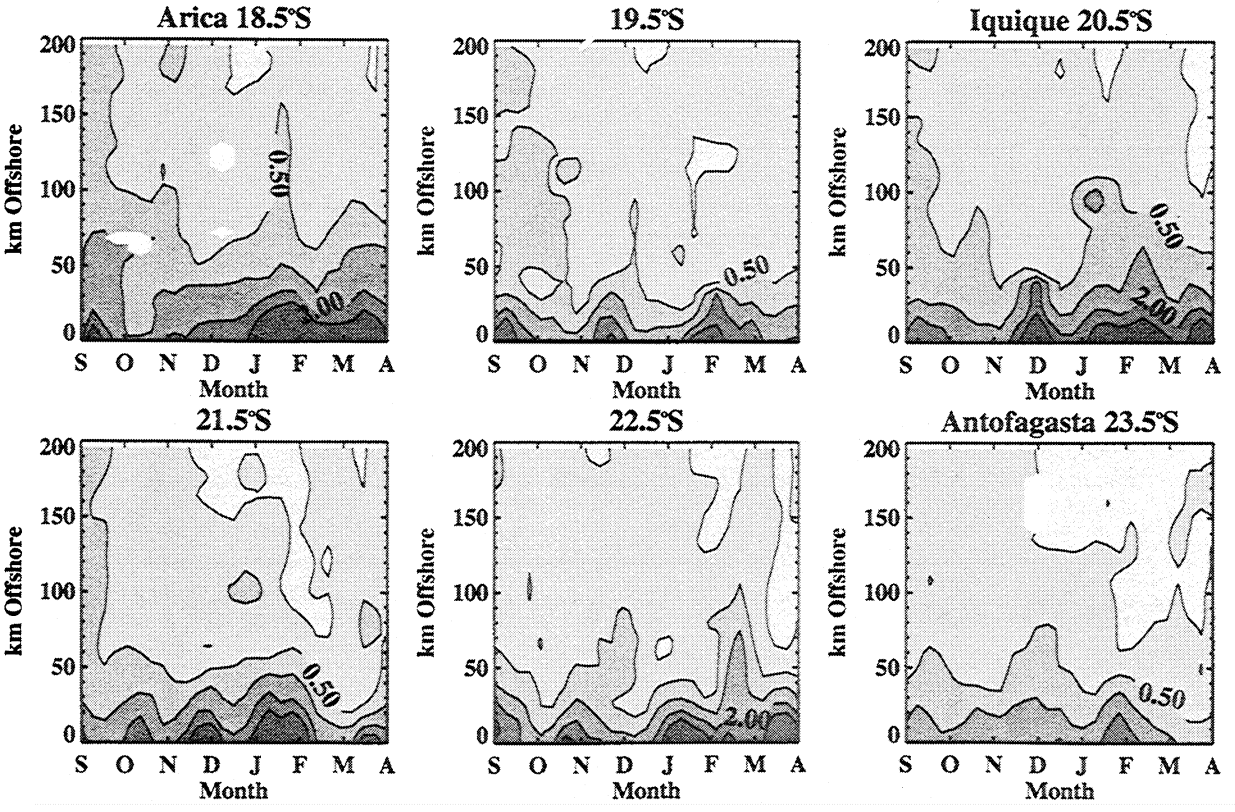

Figure 9. The distribution of SeaWiFS satellite-measured chlorophyll (mg m^{-3}) off northern Chile from September 1998 to April 1999 plotted as contours in time and cross-shelf distance at the six latitudes used in Plate 2. Data are subset from 8 day composite images with 4 km spatial resolution.

temporal patterns of chlorophyll evident in Figure 9 (non-El Niño) clearly track the temporal patterns of SST and frontal activity in 1996 (Figures 2, 4, 5c and 6b) as well as the chlorophyll patterns measured by the OCTS (Figure 8) more closely than those of the 1997-1998 El Niño period. It is also of note that the seasonal cycle evident in the (much more extensive) SeaWiFS data from 1998 to 1999 (Figure 9) as well as the OCTS data from 1996 to 1997 is out of phase with the 1979 CZCS data presented by *Thomas* [1999].

4.4. Coincident in Situ Data

Inadequacies in the atmospheric correction and/or in-water algorithm used to extract chlorophyll concentrations from the SeaWiFS data version available at present might bias the temporal and spatial patterns shown here. Precise validation of the SeaWiFS data requires specific protocols [e.g., *Mueller and Austin*, 1995] and cannot be reproduced for the time/space period analyzed here. However, spatial and temporal averages can be used to estimate, at least to a first approximation, whether general trends seem reasonable. *Chavez* [1995] uses this approach to show that climatological CZCS pigment time series capture the same large-scale cross-shelf chlorophyll seasonal cycle measured in situ off California but that systematic differences are apparent off Peru. At the time of writing, there is no doubt that the SeaWiFS data will be subjected to further reprocessing, taking advantage of improved atmospheric correction schemes, and that satellite-derived chlorophyll concentrations will continue to be improved upon.

In situ surface chlorophyll measurements coincident with the SeaWiFS data are available from a series of cruises made by IFOP to monitor oceanographic conditions during the 1997-1998 El Niño and their subsequent recovery. These data are averaged latitudinally within cross-shelf bins to provide a single mean cross-shelf profile of surface chlorophyll concentration representative of the northern Chile study area for each cruise period. In situ data from four cruises are shown in Figure 10 and compared with the latitudinally averaged cross-shelf profile extracted from the most closely coincident SeaWiFS 8 day composite. These data show three features. First, the SeaWiFS data systematically overestimate in situ surface chlorophyll in the study region by a factor of 2-4. As this paper goes to press, a complete reprocessing of the SeaWiFS data is underway, hopefully reducing this bias. Second, the SeaWiFS data successfully capture the mean relative cross-shelf structure of the chlorophyll in each cruise, with a similar bias during all four comparison periods. This suggests that despite inaccuracies in the absolute chlorophyll concentration retrieved from the SeaWiFS data, the data can be used to provide an initial view of the time and space patterns of relative chlorophyll within the study region. Third, distinct differences are apparent between available years. Comparisons of in situ data from two hemispherical summers, December 1997 (the height to El Niño conditions) and December 1998 (non-El Niño conditions), show that within the nearshore upwelling region, mean chlorophyll concentrations are significantly larger during the non-El Niño year. In December 1998 these concentrations are > 1.0 mg m^{-3} within 20 km of shore and reach a maximum of 1.5 mg m^{-3}. This provides further evidence that chlorophyll patterns during the El Niño conditions of the 1997-1998 summer are anomalous and that under more normal conditions, chlorophyll patterns would more closely resemble the time/space structure evident in the SST satellite data from 1996 (Figures 4 and 6).

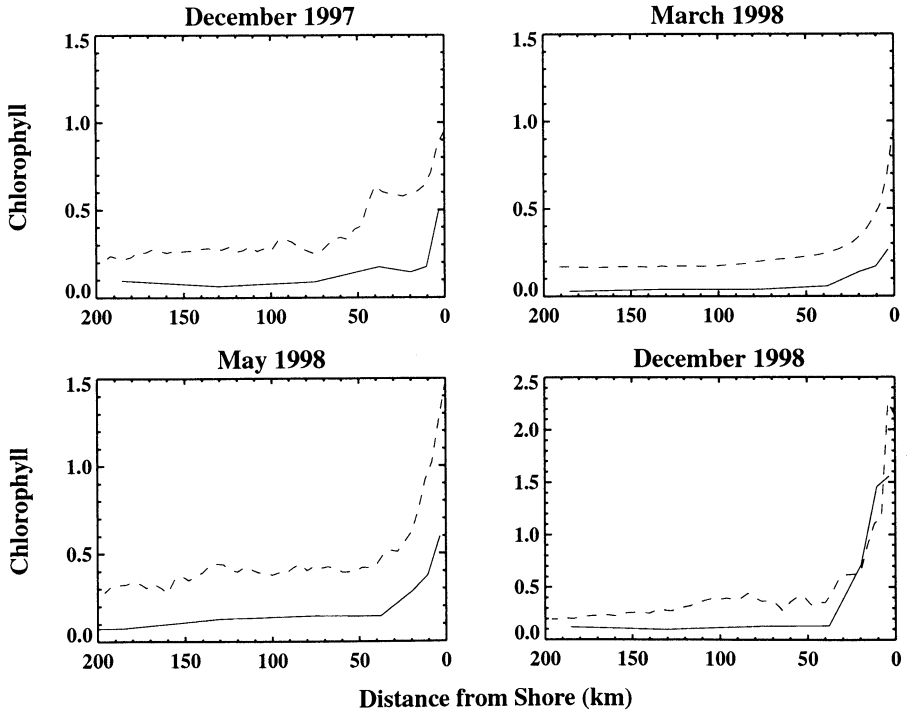

Figure 10. Latitudinally averaged cross-shelf profiles of chlorophyll off northern Chile from four time periods of in situ surface measurements (solid line) and SeaWiFS retrievals (dashed line).

5. Summary

Satellite data document the evolution of SST from the La Niña conditions of 1996 through the El Niño of 1997 and early 1998 in the upwelling region off northern Chile. These confirm the surface temperature descriptions provided by Blanco et al. (submitted manuscript, 2000) based on in situ hydrographic data but provide increased temporal and spatial resolution. SeaWiFS chlorophyll patterns beginning in September 1997 provide a first estimate of the biological response to the El Niño signal and subsequent recovery.

Comparisons to the La Niña conditions of 1996 show that the first pulse of El Niño anomalies in May 1997 (late fall) results in delayed seasonal development of austral winter SST patterns, warmer surface temperatures throughout the study region, and an earlier and more prolonged winter minimum of coastal SST deficit but little detectable difference in frontal structure. The second pulse in December 1997, however, arrives in late spring-early summer, resulting in increased SST and reduced frontal structure and coastal deficit throughout in the study area. These conditions begin to subside in March 1998 such that by April-May (fall), SST frontal structure and coastal deficit are similar to those of 1996 and early 1997.

Chlorophyll patterns show that both concentrations within the upwelling region and cross-shelf extension of elevated concentrations increase in October and November 1997, during the relaxation between El Niño pulses, to > 3.0 mg m^{-3} with values of 1.0 mg m^{-3} extending up to 50 km offshore. In early December, at the time of the arrival of the second pulse both metrics of chlorophyll become strongly reduced, and concentrations are < 0.5 mg m^{-3} even immediately adjacent to the coast throughout most of the study area. Low concentrations persist throughout austral summer until April (fall), when concentrations nearshore increase above 1.0 mg m^{-3} and the 0.5 mg m^{-3} isoline begins to expand offshore to reach a seasonal maximum in winter (August) 1998 > 200 km offshore.

The extent to which SeaWiFS-measured chlorophyll concentrations and patterns during the 1997-1998 El Niño period are anomalous awaits a longer time series of data. In situ surface chlorophyll measurements show that SeaWiFS retrievals may be high by a factor of 2-4, but consistency in this bias indicates that the relative patterns over time are valid. The consistent covariability of SST and chlorophyll data during the El Niño period suggests a close linkage between the temporal evolution of biological spatial patterns and SST structure. The time series of cross-shelf chlorophyll closely tracks both the strength and the cross-shelf position of SST frontal zones associated with upwelling features as well the SST index of upwelling. If similar relationships between surface biological and physical conditions existed during the 1996 cold La Niña, phase of the ENSO cycle, available AVHRR data from this period suggest higher summer coastal concentrations and an increased width of the coastal high-biomass region. These expected differences are supported by OCTS data from 1996-1997, noncoincident in situ data from the study region, and SeaWiFS data from the following (non-El Niño) year.

Acknowledgments. SeaWiFS level 2 data are made available by the Goddard Space Flight Center DAAC. We thank Mark Abbott for helpful suggestions. Funding for ACT came from NASA grants NAG5-6558 and NAG5-6604 and NSF grant OCE-9711919 (part of the U.S. GLOBEC program). Data collection and support for JLB and JO was provided by IFOP, with funding by Fondo de Investigacion Pesquera (Projects 95-05, 96-07 and 97-02). Funding for MEC was provided by the NASA Ocean Biogeochemistry Program and for PTS by JPL grant 958128 (TOPEX) and NASA grants NAG5-4947 (EOS) and NAG5-6604. Additional funding for travel for all authors to collaborate in the analysis of these data came from NASA and an NSF supplement to grant OC-9711344 (part of the U.S. GLOBEC program).

References

Abbott, M.R., and P.M. Zion, Satellite observations of phytoplankton variability during an upwelling event, *Cont. Shelf Res., 4*, 661-680, 1985.

Arnone, R.A., and P.E. LaViolette, Satellite definition of the bio-optical and thermal variation of coastal eddies associated with the African Current, *J. Geophys. Res., 91*, 2351-2364, 1986.

Barber, R.T., and F.P. Chavez, Biological consequences of El Niño, *Science, 222*, 1203-1210, 1983.

Barber, R.T., and F.P. Chavez, Ocean variability in relation to living resources during the 1982-83 El Niño, *Nature, 319*, 279-285, 1986.

Barbieri, M.A., M. Bravo, M. Farias, A. Gonzalez, O. Pizarro, and E. Yáñez, Phenomena associated with the sea surface thermal structure observed through satellite images in northern Chile, *Invest. Mar. Valparaiso, 23*, 99-122, 1995.

Blanco, J.L., A.C. Thomas, M.-E. Carr, and P.T. Strub, Seasonal climatology of hydrographic conditions in the upwelling region off northern Chile. *J. Geophys. Res.*, in press, 2000.

Campbell, J.W., J.M. Blaisdell, and M. Darzi, Level-3 SeaWiFS data products: Spatial and temporal binning algorithms, NASA Tech. Memo., *104566*, vol. 32, 73 pp., 1995.

Chavez, F.P., A comparison of ship and satellite chlorophyll from California and Peru, *J. Geophys. Res., 100*, 24,855-24,862, 1995.

Chavez, F.P., P.G. Strutton, and M.J. McPhaden, Biological-physical coupling in the central equatorial Pacific during the onset of the 1997-1998, *Geophys. Res. Lett., 25*, 3543-3546, 1998.

Enfield, D.B., El Niño, past and present. *Rev. Geophys., 27*, 159-187, 1989.

Enfield, D.B., M.P. Cornejo-Rodriguez, R.L. Smith, and P.A. Newberger, The equatorial source of propagating variability along the Peru coast during the 1982-1983, *J. Geophys. Res., 92*, 14,335-14,346, 1987.

Fonseca, T., and M. Farias, Estudio del proceso de surgencia en la costa chilena utilizando percepcion remota, *Invest. Pesq. Chile, 34*, 33-46, 1987.

Hill, A.E., B.M. Hickey, F.A. Shillington, P.T. Strub, K.H. Brink, E.D. Barton, and A.C. Thomas, Eastern boundary currents: A pan-regional review, in: *The Sea,* Vol. 11, edited by A.R. Robinson and K.H. Brink, pp. 29-68, John Wiley, New York, 1998.

Hood, R.R., M.R. Abbott, and A. Huyer, Phytoplankton and photosynthetic light response in the coastal transition zone off northern California in June 1987, *J. Geophys. Res., 96*, 14,769-14,780, 1991.

Huyer, A., and R.L. Smith, The signature of El Niño off Oregon in 1982-83, *J. Geophys. Res., 90*, 7133-7142, 1985.

Huyer, A., R.L. Smith, and T. Paluszkiewicz, Coastal upwelling off Peru during normal and El Niño times, 1981-1984, *J. Geophys. Res., 92*, 14,297-14,307, 1987.

Huyer, A., M. Knoll, T. Paluszkiewicz, and R.L. Smith, The Peru undercurrent: A study in variability, *Deep Sea Res., Part A, 38*, S247-S271, 1991.

Morales, C.E., J.L. Blanco, M. Braun, H. Reyes, and N. Silva, Chlorophyll-*a* distribution and associated oceanographic conditions in the upwelling region off northern Chile during the winter and spring 1993, *Deep Sea Res.*, Part A, *43*, 267-289, 1996.

Mueller, J.L., and R.W. Austin, Ocean optics protocols for SeaWiFS validation, NASA Tech. Memo., *104566*, vol. 25, 67 pp., 1995.

Philander, S.G., *El Niño, La Niña, and the Southern Oscillation*, 289 pp., Academic, San Diego, Calif., 1990.

Reinecker, M.M., and C.N.K. Mooers, The 1982-83 El Niño signal off northern California, *J. Geophys. Res., 91*, 6597-6608, 1986.

Rojas, R., and N. Silva, *Atlas Oceanográfico de Chile,* vol. 1, Serv.

Hidrogr. y Oceanogr. de la Armada de Chile, Valparaíso, Chile, 1996.

Shaffer, G., O. Pizarro, L. Djurfeldt, S. Salinas, and J. Rutllant, Circulation and low-frequency variability near the Chilean coast: Remotely forced fluctuations during the 1991-1992 El Niño, *J. Phys. Oceanogr.*, *27*, 217-235, 1997.

Strub, P.T., C. James, A.C. Thomas, and M.R. Abbott. Seasonal and non-seasonal variability of satellite derived surface pigment concentration in the California Current, *J. Geophys. Res. 95*, 11,501-11,530, 1990.

Strub, P.T., P.M. Kosro, and A. Huyer, The nature of the cold filaments in the California Current system, *J. Geophys. Res.*, *96*, 14,743-14,768, 1991.

Strub, P.T., J. Mesias, V. Montecino B., J. Rutllant C., and S.S. Marchant, Coastal ocean circulation off western South America, in: *The Sea,* Vol. 11, edited by A.R. Robinson and K.H. Brink, pp. 273-314, John Wiley, New York, 1998.

Thomas, A.C., Seasonal distributions of satellite-measured phytoplankton pigment concentration along the Chilean coast,*J. Geophys. Res.*, *104*, 25,877–25,890, 1999.

Thomas, A.C., F. Huang, P.T. Strub, and C. James, A comparison of the seasonal and interannual variability of phytoplankton pigment concentrations in the Peru and California Current System, *J. Geophys. Res., 99*, 7355-7370, 1994.

Thomas, A.C., and P.T. Strub, Seasonal and interannual variability of pigment concentrations across a California Current frontal zone, *J. Geophys. Res.*, *95*, 13,023-13,042, 1990.

Van Camp, L., L. Nykjaer, E. Mittelstaedt, and P. Schlittenhardt, Upwelling and boundary circulation off northwest Africa as depicted by infrared and visible satellite observations, *Prog. Oceanogr.*, *26*, 357-402, 1991.

Yanez, E., A. Gonzalez, and M.A. Barbieri, Sea surface thermal structure associated to the space-temporal distribution of sardine and anchovy in northern Chile,*Invest. Mar. Valparaiso, 23*, 123-147, 1995.

J.L. Blanco and J. Osses, Instituto de Fomento Pesquero, Casilla 8-V, Valparaíso, Chile. (jlblanco@ifop.cl; josses@ifop.cl)

M.E. Carr, Jet Propulsion Laboratory, California Institute of Technology, MS 300-323, 4800 Oak Grove Dr., Pasadena, CA 91009-8099 (mec@pacific.jpl.nasa.gov)

P.T. Strub, College of Oceanic and Atmospheric Sciences, Oregon State University, Corvallis, OR 97331-5503 (tstrub@oce.orst.edu)

A.C. Thomas, School of Marine Sciences, University of Maine, Orono, ME 04469-5741 (thomas@maine.edu)

(Received August 30, 1999; revised July 10, 2000;
accepted July 27, 2000)